University of Baghdad
College of Engineering
JE
JOURNAL OF ENGINEERING

Journal of Engineering

journal homepage: www.jcoeng.edu.iq

Volume 31 Number 7 July 2025

Seismic Performance of Reinforced Concrete Non-Prismatic Columns

Jabbar Abdalaali Kadhim *, **Salah R. Al.Zaidee**, **Hayder Amer Al-Baghdadi**

Department of Civil Engineering, College of Engineering, University of Baghdad, Baghdad, Iraq

ABSTRACT

This paper investigates the potential enhancement of the seismic performance of reinforced concrete square columns by modifying their geometry from prismatic to non-prismatic, while maintaining the same volume. Two one-bay by two-bay three-story RC frames were simulated using ABAQUS software; the first has prismatic columns serving as the reference model, and the second has non-prismatic columns. Static lateral loads were applied to both frames after the application of gravity loads. Additionally, two one-bay by one-bay six-story RC buildings were modeled in ABAQUS; one has prismatic columns and the other has non-prismatic columns. These two models were subjected to the El Centro 0.32g NS 1940 earthquake, and time-history analyses were performed. The results showed that the seismic response, in terms of base shear capacity and stiffness, was significantly improved in the case of columns linearly tapered from a smaller cross-section at mid-height to a larger cross-section at the ends. For a tapering angle of 3.814°, the lateral strength increased by 56.4%, and the initial stiffness improved by 50.5%. Moreover, the overstrength factor of the RC frame with tapered columns increased by 56.48% compared to the prismatic-column reference model. The damage pattern in the frame with non-prismatic columns was also more favorable than that of the reference frame.

Keywords: Non-prismatic, Reinforced concrete, Columns, Seismic, Damage.

1. INTRODUCTION

In seismic design, structural engineers aim to ensure that buildings achieve acceptable performance levels during probable future earthquakes while minimizing construction costs **(Gharehbaghi et al., 2016)**. The traditional seismic design process for Reinforced Concrete (RC) structures is illustrated in **Fig. 1 (Arroyo and Gutierrez, 2017).** Following the design steps shown in **Fig. 1**, the structural engineer may conduct design iterations to achieve an acceptable design that satisfies both strength and drift requirements. Although the design achieved complies with the code requirements, it may not be the most optimal design from

*Corresponding author
Peer review under the responsibility of University of Baghdad.
https://doi.org/10.31026/j.eng.2025.07.03
This is an open access article under the CC BY 4 license (http://creativecommons.org/licenses/by/4.0/).
Article received: 26/09/2024
Article revised: 09/05/2025
Article accepted: 04/06/2025
Article published: 01/07/2025

an economic point of view. Therefore, the problem of design optimization has arisen. On the other hand, without employing powerful developments in computer science and computational techniques, design optimization is heavy and complicated to achieve. Thus, several computer-automated methods have been proposed to optimize the seismic design of RC structures.

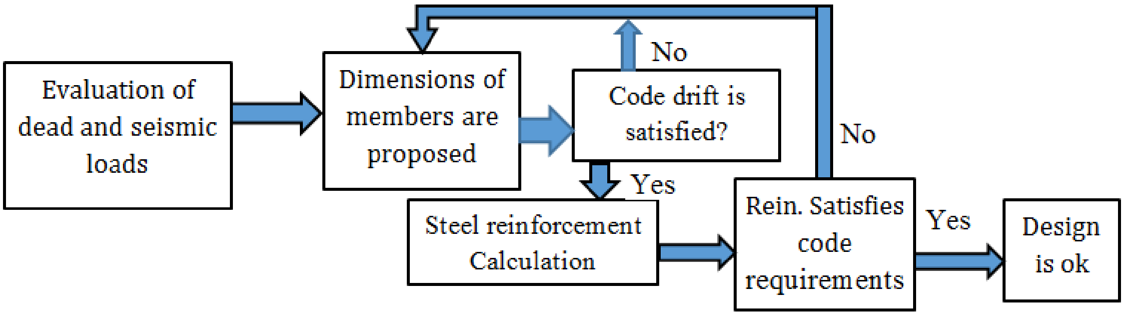

Figure 1. Typical process of traditional seismic design of RC structures **(Arroyo and Gutierrez, 2017)**.

Structural design optimization is performed by minimizing or maximizing one or more objective functions, while satisfying a set of predefined constraints **(Faidh-Allah and Kadem, 2011; Tanhadoust et al., 2023; Zakian and Kaveh, 2023)**. The objective functions are the weight of the structure, construction cost, seismic input energy, hysteretic energy dissipation, and others. Most design optimization studies adopt the cost of the structure as the objective function **(Kaveh and Zakian, 2014; Hu, 2021; Jebelli and Behnam, 2024)**. The weight of the structure was adopted to optimize the design of steel communication towers **(Said and Hashim, 2013)**. The efficient design of frame buildings, whether they are steel or RC structures, has been a continual focus of research for several decades. Steel structures typically have a limited number of design variables, whereas the optimal design of RC structures involves more design variables and constraints. The efficient design of frame buildings, whether they are steel or reinforced concrete (RC) structures, has been a continual focus of research for several decades. Steel structures typically have a limited number of design variables, whereas the optimal design of RC structures involves a variety of design variables and constraints **(Behbahan, 2012)**. However, recent studies have been introduced to establish frameworks and computational techniques for solving the problem of the optimum design of RC structures.

Advancements in the design optimization of RC structures have embraced various techniques to address the challenge of achieving optimal designs. These techniques encompass linear and non-Linear Programming and the application of optimality criteria methods utilized to attain the best design solutions for RC frame structures under static loads **(Krishnamoorthy and Munro, 1973; Balling and Yao, 1997; Fadaee and Grierson, 1998)**. On the other hand, the optimum seismic design of RC structures has taken a notable interest worldwide **(Zou and Chan, 2005; Fragiadakis and Papadrakakis, 2008).** In performance-based seismic design, the control of the interstory drift is a main objective for the structural engineer **(Zou and Chan, 2004)**. The interstory drift, defined as the difference in lateral deflection between the top and bottom of the considered story, must be limited to the values prescribed by the codes. Satisfying this crucial requirement ensures a properly designed structure with adequate stiffness and strength **(Taranath, 2004).**

This study aims to investigate the potential for optimizing the structural behavior of RC columns by changing their geometry from prismatic to non-prismatic. In the proposed non-prismatic design, the volume of concrete used in the prismatic reference column is maintained, while the design is reassessed using non-prismatic columns. The non-prismatic columns considered in this study are linearly tapered from mid-height toward the column ends. The slenderness ratio of RC linearly tapered columns can be evaluated based on the average cross-section **(Brant, 1984; Kadhim and Al-Zaidee, 2024)**.
Four RC frames were modeled using ABAQUS software; two reference building models have prismatic columns, and the others have tapered ones. The numerical modeling has been validated in a previous study by the comparison between the numerical results and the experimental results of testing RC columns. Two tapered columns tested by **(Brant, 1984)** were simulated numerically. The numerical failure loads were 100.125% and 99.297% of the corresponding experimental failure loads, indicating excellent agreement. Additionally, the load-displacement relationships showed good correlation between the numerical and experimental results. Therefore, the validity of the numerical modeling is confirmed **(Kadhim and Al-Zaidee, 2023)**. Constitutive relationships of materials, parameters of concrete damaged plasticity, and parameters of tension stiffening have been detailed and described in the aforementioned study. It has been found that using the concrete damaged plasticity model in ABAQUS leads to good agreement between numerical and experimental results **(Mahmoud and Al-Baghdadi, 2018)**.

2. SEISMIC ANALYSIS PROCEDURE

According to ASCE/SEI 7-16 standard (minimum design loads for buildings and other structures), all of the analysis procedures for the structures subjected to seismic loads are permitted to analyze structures without structural irregularities and not more than 48.8 m in height. This height limitation is due to that the procedure of equivalent static lateral force becomes unrealistic for higher buildings because of the significant contributions of higher modes to the seismic response of such buildings. The nonlinear time-history and equivalent static force analyses were used in the present study to obtain the structural responses of the modeled RC frames. The equivalent lateral force procedure is a simplified method that estimates the natural period for the structural system and uses the expected maximum ground acceleration and other relevant factors to evaluate the base shear **(Abbas and Abdulhameed, 2019)**. In this procedure, only the first mode of the structure is considered, and the contributions of higher modes are neglected, as their influence on the structural response is negligible **(Manohar and Madhekar, 2015; Hejazi and Tan, 2020)**.
In the lateral force procedure, the simplified design procedure presented in ASCE 7 is permitted to evaluate the total base shear in the considered direction according to the International Building Code (IBC) **(ICC, 2015)**. The total base shear, based on the aforementioned procedure, is calculated as follows **(ASCE/SEI, 2016):**

$$V = C_s\, W \tag{1}$$

Where
C_s = the seismic response coefficient.
W= the effective seismic weight of the structure.
The seismic response coefficient is calculated as follows :

$$C_s = \frac{S_{DS}}{(R/I)} \tag{2}$$

Where S_{DS} is the design response spectral acceleration at the short period, R is the response modification factor, and I is the importance coefficient. For moment-resisting concrete frames, R has the values as given in **Table 1**.

Table 1. Response modification factor for RC moment frames **(ASCE/SEI, 2016).**

Seismic force-resisting system	Response modification coefficient (R)
Special RC moment frame	8
Intermediate RC moment frame	5
Ordinary RC moment frame	3

The vertical distribution of the base shear is as given in Eq. (3).

$$F_x = C_{vx} V \tag{3}$$

Where F_x is the is the force applied at level x, C_{vx} is the factor of the vertical distribution, and V is the total base shear. C_{vx} is given by Eq. (4) as follows:

$$C_{vx} = \frac{w_x h_x^k}{\sum_1^n w_i h_i} \tag{4}$$

Where w_x is the portion of the total weight (W) at the level x, h_x is the distance from the base to the level x, k is an exponent depending on the time period of the structure. w_i is the portion of the total weight (W) at level i, and h_i is the distance from the base to the level i.

3. RC FRAMES SUBJECTED TO STATIC LATERAL LOADS

3.1 Frame A

Frame A is a three-story, one-bay by two-bay RC frame with prismatic columns, as shown in **Fig. 3**. The clear height of the columns is 3 meters. The proposed non-prismatic column geometry is expected to enhance both lateral stiffness and lateral strength. Therefore, the behavior of RC frames with additional bays and/or stories is anticipated to be similar to that observed in the studied numerical models. **Fig. 4** shows the cross-sections of the six prismatic columns and the beams.

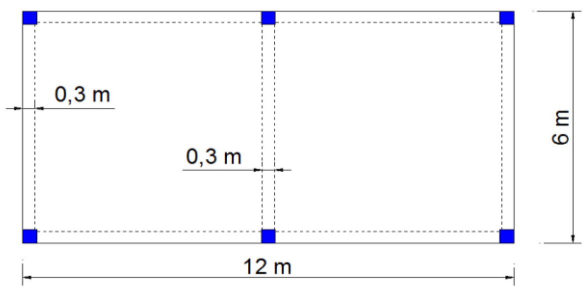

Figure 3. The plan of Frame A.

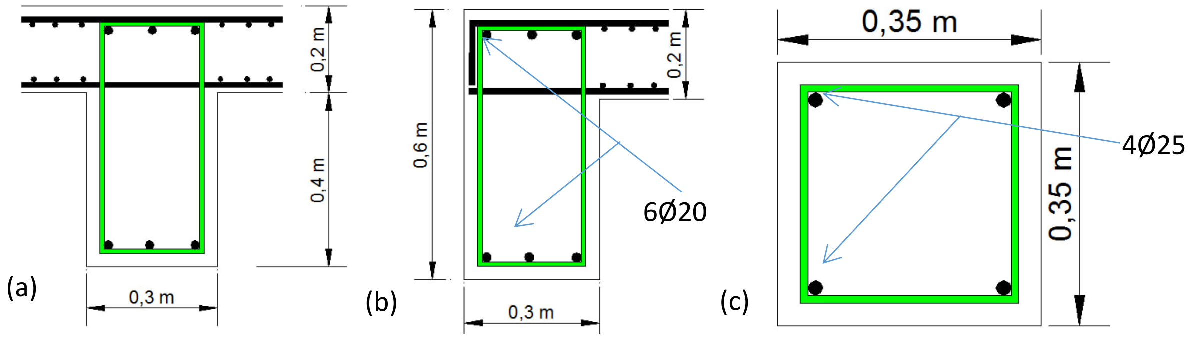

Figure 4. (a) Cross-section of interior beams, (b) cross-section of exterior beams, and (c) cross-section of prismatic columns of Frame A.

The Finite Element (FE) model of the frame is shown in **Fig. 5**. A mesh sensitivity analysis was conducted to evaluate the influence of element size on the accuracy and stability of the numerical results. Through this process, it was determined that using a continuum element length of 60 mm provides a suitable balance between computational efficiency and solution accuracy. As a result, this element size was adopted for the finite element model in the subsequent analyses. **(Kadhim and Al-Zaidee, 2023)**.

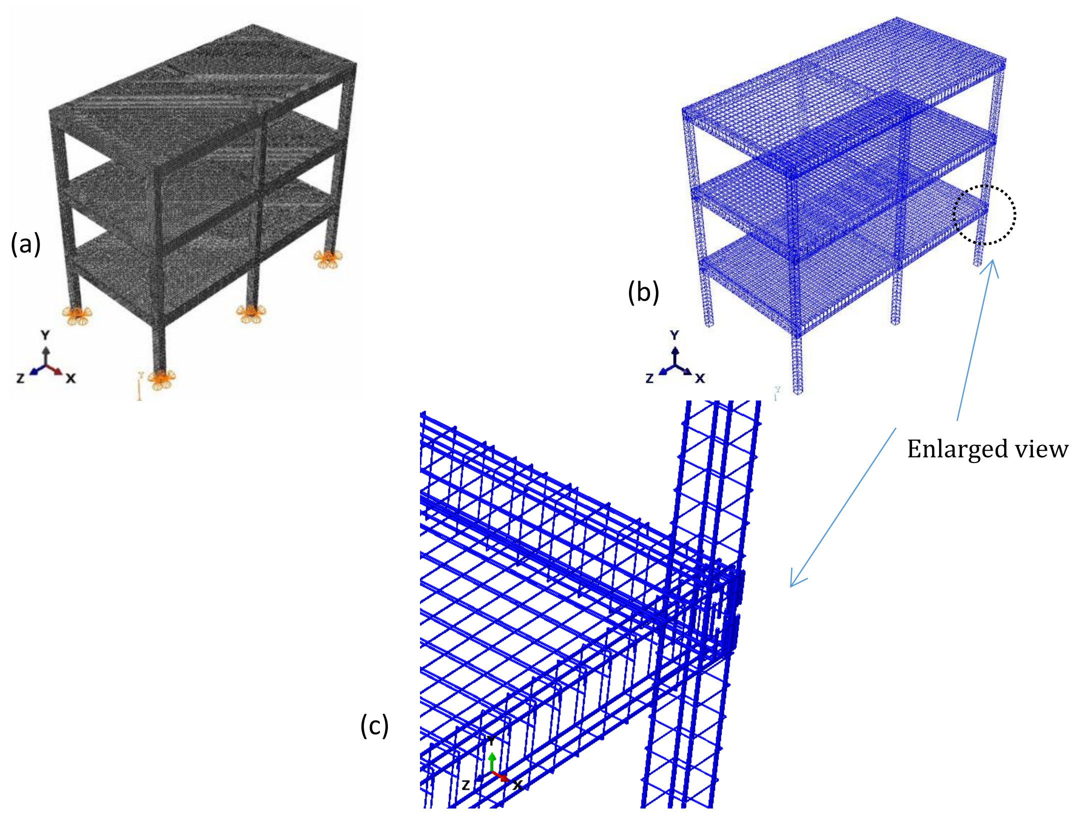

Figure 5. FE model, (a). concrete continuum elements, (b). truss elements, and ©. enlarged view of reinforcement of Frame A.

The model was analyzed under gravity load and lateral static loads applied at floor levels. The gravity load was applied in the first load step as a downward-directed gravitational acceleration. Since the material mass densities were defined, the software automatically converted the acceleration into equivalent nodal forces. In the second load step, static lateral loads were introduced as horizontal pressures at each floor level. The bases of the columns were fully fixed by restraining all degrees of freedom at their bottom cross-sections. The static lateral loads were applied in the long direction, and the nonlinear static analysis was performed. The values of the lateral loads at different levels were proportionally consistent with the vertical distribution of the base shear given in Eq. (4). **Fig. 6** shows the application of gravity and lateral loads. **Fig. 7** shows the cracks pattern in the model of Frame A, while **Fig. 8** illustrates the stresses in the steel reinforcement.

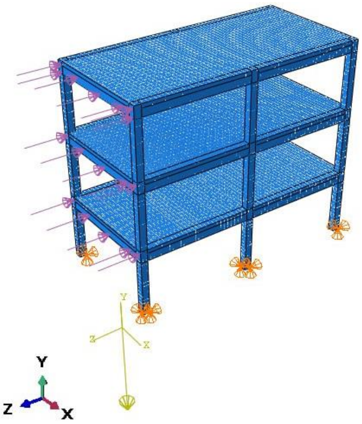

Figure 6. Application of gravity and lateral loads to Frame A.

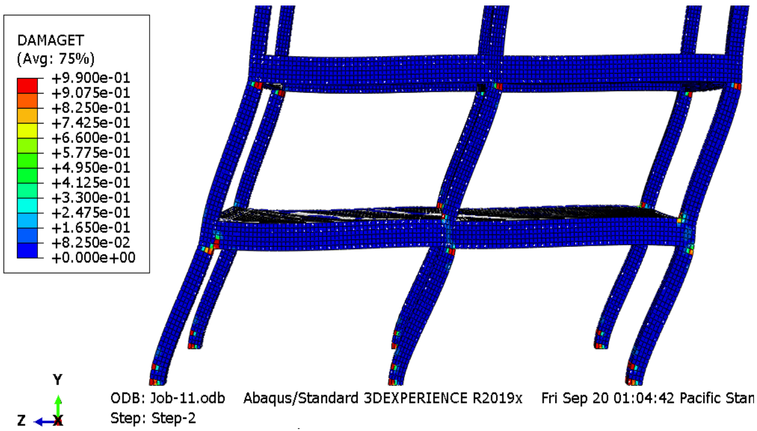

Figure 7. Tensile cracks in the model of RC Fame A.

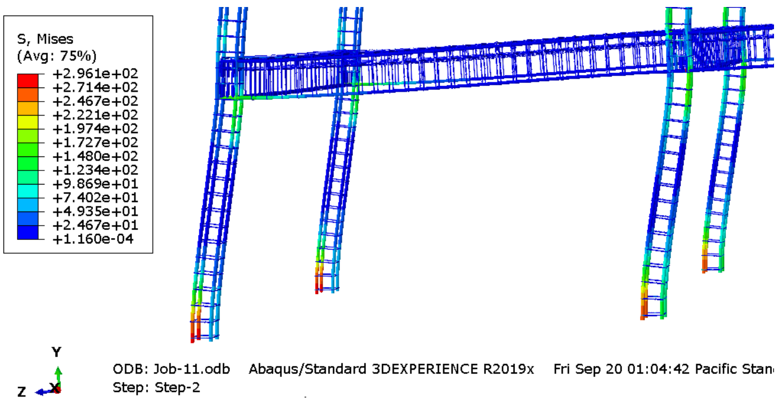

Figure 8. Stresses in reinforcement of Frame A.

3.2 Frame B

Frame B is an RC frame similar to Frame A, with the only difference being that the columns are non-prismatic. In Frame B, the columns are tapered from (250×250) mm at mid-height to (450×450) mm at the ends. Thus, the tapering angle, which is the inclination of the column side faces, is 3.814°. Under lateral loads, and by neglecting the variation in shear force within the story height, the mid-height points of the columns represent points of contraflexure. For this reason, the current study proposes shifting part of the concrete material toward the column ends to increase the moment capacity at locations of higher bending moments. Evaluating the volume of a tapered column based on the average cross-section does not result in a volume exactly equivalent to that of the reference prismatic column; hence, a small difference is neglected. **Fig. 9** shows the FE model of Frame B. The longitudinal reinforcement of columns are parallel to the inclined column edges, as can be seen in **Fig. 9.b**.

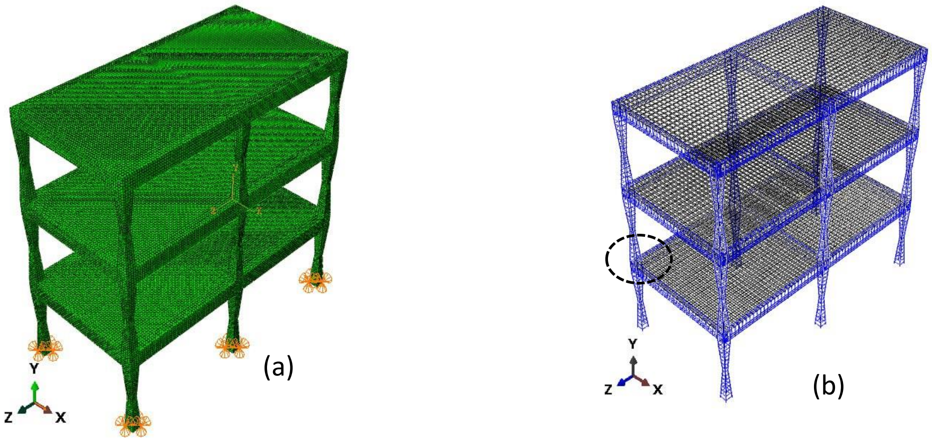

Figure 9. FE model of Frame B: (a) concrete continuum elements, and (b) truss elements.

Fig. 10 shows an enlarged view for the reinforcement of the model (the truss elements). The tensile cracks in the model of Frame B are as demonstrated in **Fig. 11**. **Fig. 12** shows the stresses in the steel reinforcement of the model. **Fig. 13** depicts the lateral load versus lateral displacement at the first floor for both Frame A and B.

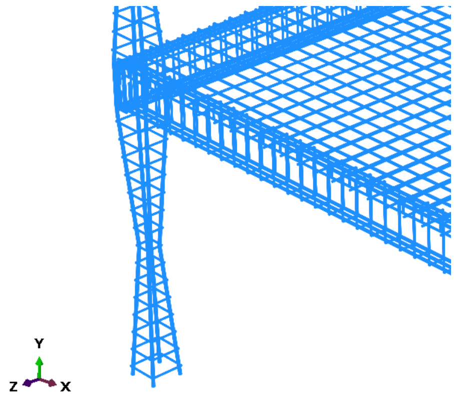

Figure 10. Enlarged view of the reinforcement of the model of RC Frame B.

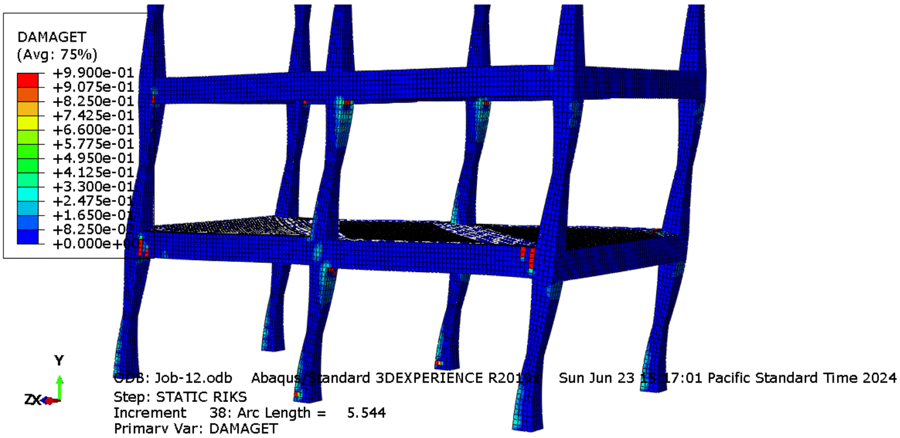

Figure 11. Tensile cracks in the model of RC Fame B.

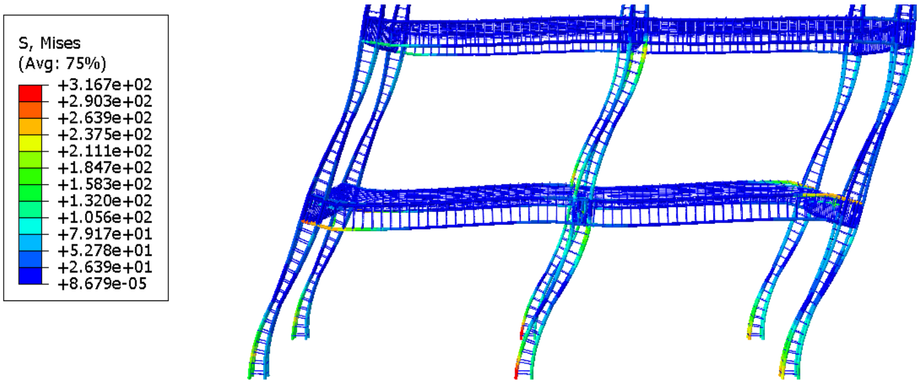

Figure 12. Stresses in reinforcement of Frame A.

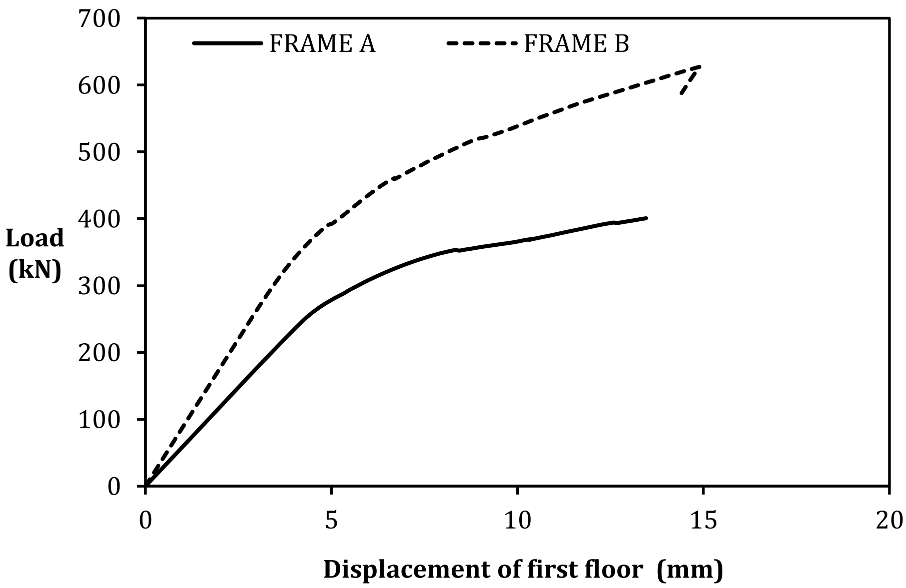

Figure 13. Numerical lateral load-displacement relationships of Frames A and B.

It can be seen, from **Fig. 13**, that the seismic behavior of Frame B is notably better that that of Frame A. The failure load of Frame A is 400.7 kN, while it is 627 kN for Frame B. The initial stiffness of the frame A is 58.47 kN/mm, but it is 88 kN/mm. Thus, tapering the columns from mid height to ends, with a tapering angle of 3.814o, enhanced the lateral strength by 56.4% and the initial stiffness by 50.5%. But, this is correct to some extent of the value of the tapering angle. Verifying the optimum value of the tapering angle is out of the scope of this study.
Structures constructed in Baghdad region are assigned to the Seismic Design Category (SDC) A according to the IBC Code (2000) **(Fattah and Al-Tae'e, 2004).** According to the Iraqi seismic Code (2017), the simplified analysis procedure is permitted for structures assigned to SDC A. Thus, knowing that the total weight (W) for each of Frames A and B is 1310 kN, the lateral design force (V) is as follows:

$$V = \frac{1.2\, S_{DS}}{R}\, W \tag{5}$$

Where S_{DS} is the design spectral response acceleration parameter in the short period range, which is equal to 0.16 for Baghdad region. For Ordinary RC moment frames, Table 1 gives that R is 3. Accordingly, V is calculated as follows:

$$V = \frac{1.2\times 0.16}{3} \times 1310 = 83.84 \ \text{kN} \tag{6}$$

The overstrength factor (Ω_o) is defined as the ratio of the provided strength to the required strength **(Chen and Lui, 2005; Annan et al., 2008; El-Nashai and Di Sarno, 2015; Sucuoglu and Akkar, 2014)**. Thus, the overstrength factor for Frame A is 400.7/83.84 = 4.78, whereas in Frame B, it is 627/83.84 = 7.48. Hence, the non-prismatic columns in Frame B increased the overstrength factor by 56.48%.

4. TIME-HISTORY ANALYSIS OF RC FRAMES

Two six-story RC frames were analyzed; the first frame is Frame C, which has prismatic columns as a reference model, and the second one, named Frame D, has non-prismatic columns. The non-prismatic columns of the second frame have the same volume as that of the columns in the reference model. The two models were subjected to accelerogram of El Centro 0.32g NS 1940 ground motion, shown in **Fig. 14**, and the nonlinear time-history analyses were performed. The gravity load was applied in the first load step in ABAQUS.

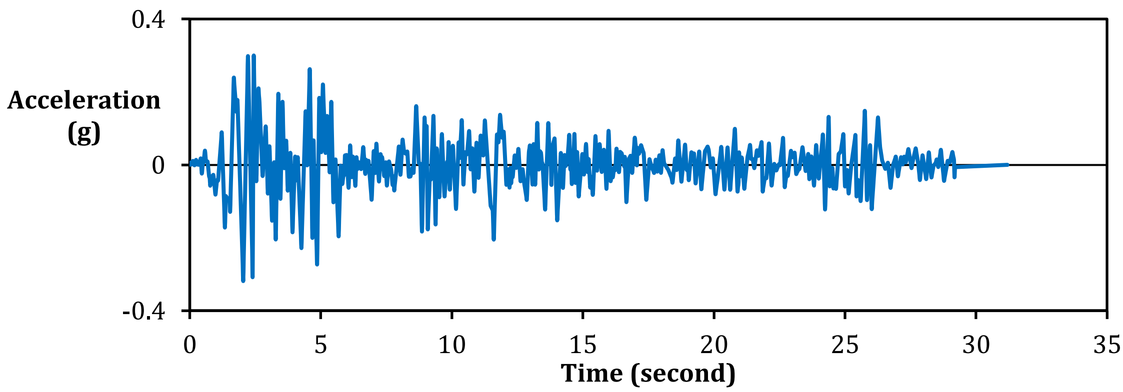

Figure 14. Accelerogram of the El Centro 0.32g 1940 NS ground motion **(Chopra, 2012)**.

4.1 Frame C

Frame C is a one-bay by one-bay six-story RC frame whose plan is shown in **Fig. 15**. The columns' cross section is (500×500) mm, and their main reinforcement is 4 ϕ 25 mm. The beams are identical to those in Frames A and B. The transverse reinforcement of columns is ϕ 10 mm at 200 mm ties. The model was subjected to the acceleration time-history, shown in **Fig. 14**, and a nonlinear time-history analysis was performed in ABAQUS. The gravity load was applied as a downward-directed gravitational acceleration in the first load step. The earthquake acceleration was then applied in the z-direction at the nodes on the bottom faces of the columns, the direction in which the structure is free to move, while all other degrees of freedom at these nodes were restrained.

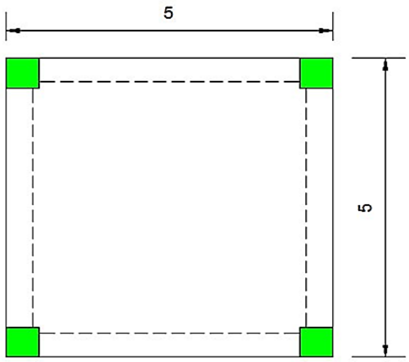

Figure 15. Plan of RC Frame C.

The Rayleigh damping model was used, in which, the mass-proportional coefficient α and the stiffness-proportional coefficient β are used to construct the damping matrix **(Bai, 2019).** These two coefficients are evaluated for a frequency-independent damping ratio as follows:

$$\alpha = \frac{2\zeta\omega_1\omega_2}{\omega_1+\omega_2} \tag{7}$$

$$\beta = \frac{2\zeta}{\omega_1+\omega_2} \tag{8}$$

Where ζ is the damping ratio, which was taken as 5%, ω_1 is the fundamental frequency of the structure, and ω_2 is the frequency of the higher mode of the structure. A frequency analysis was performed, yielding ω_1 and ω_2 as 1.929 and 21.074 cycles per second, respectively. Consequently, α and β were taken as 1.11 and 0.00069, respectively. The displacement and base shear responses are presented in **Figs. 16** and **17**, respectively,

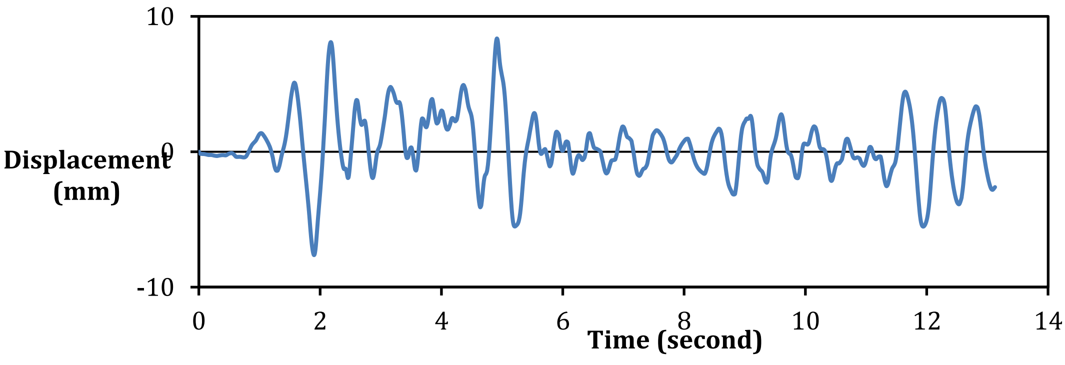

Figure 16. Displacement response at first floor level of Frame C under the effect of the El Centro 0.32g 1940 NS.

while the damage resulting from the applied ground motion is illustrated in **Fig. 18**.

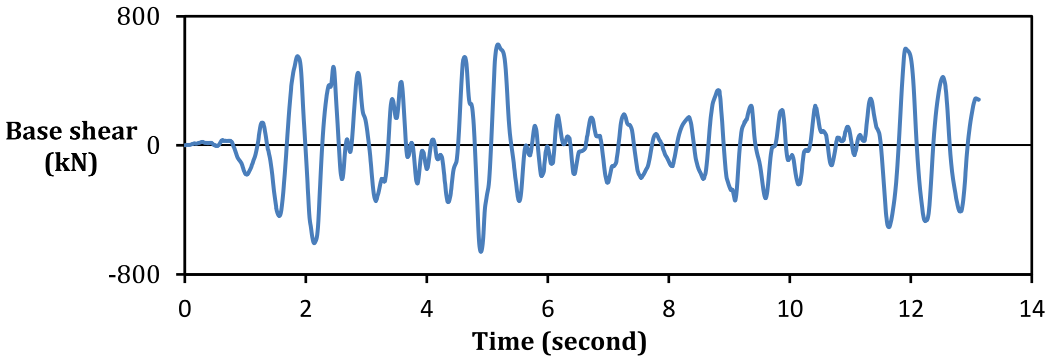

Figure 17. Base shear of model of Frame C under the El Centro 0.32g 1940 NS.

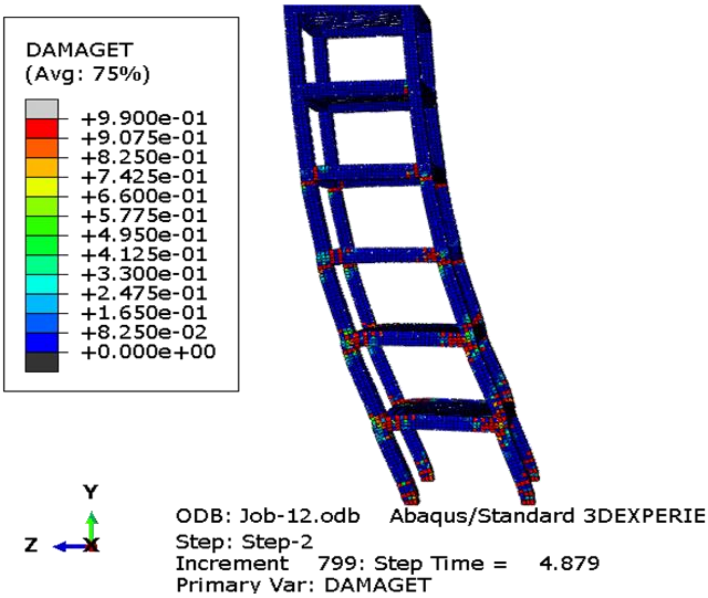

Figure 18. Damages of Frame C under the El Centro 0.32g NS 1940.

4.2 Frame D

Frame D is identical to Frame C, except that the columns in Frame F are tapered from mid-height toward the ends, maintaining the same volume as the columns in Frame E. The columns in Frame F are tapered from (350×350) mm at mid-height to (650×650) mm at the ends. Hence, the tapering angle is 5.71°. The model of Frame D was analyzed under the effect of the El Centro 0.32g excitation. **Fig. 19** shows the numerical displacement responses of Frames C and D, and the base shear of Frame D is shown in **Fig. 20**. The damages are shown in **Fig. 21**.

In seismic design of RC structures, it is aimed to make the formation of plastic hinges occur first at the ends of beams rather than the columns **(Derecho and Kianoush, 2001; Fragiadakis and Papadrakakis, 2008; Nie et al., 2020)**. More capability of energy dissipation can be provided by the beam-sway mechanism **(Dooley and Bracci, 2001; Sunitha et al., 2014; Bai and Ou, 2015)**. Post-earthquake observations have shown that the main cause of the collapse of RC structures is the failure of columns **(Chen et al., 2016)**.

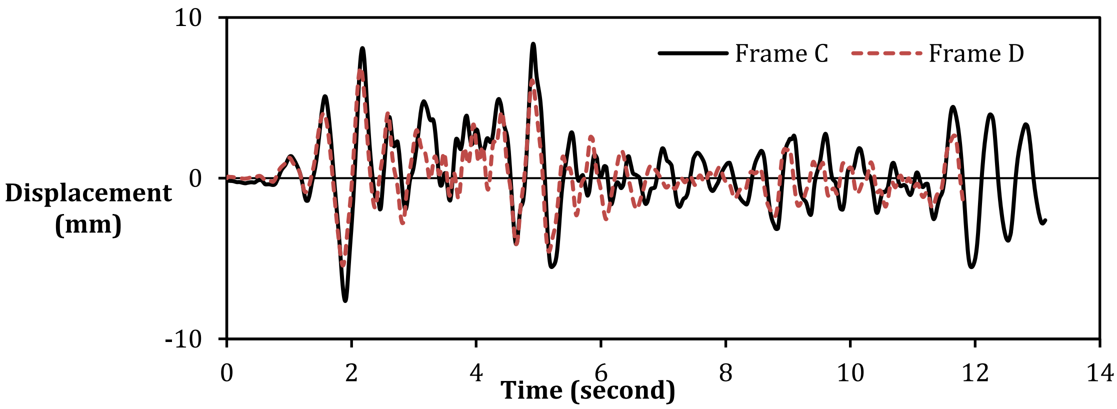

Figure 19. Displacement responses at first floor level of Frames C and D for the El Centro 0.32g 1940 NS.

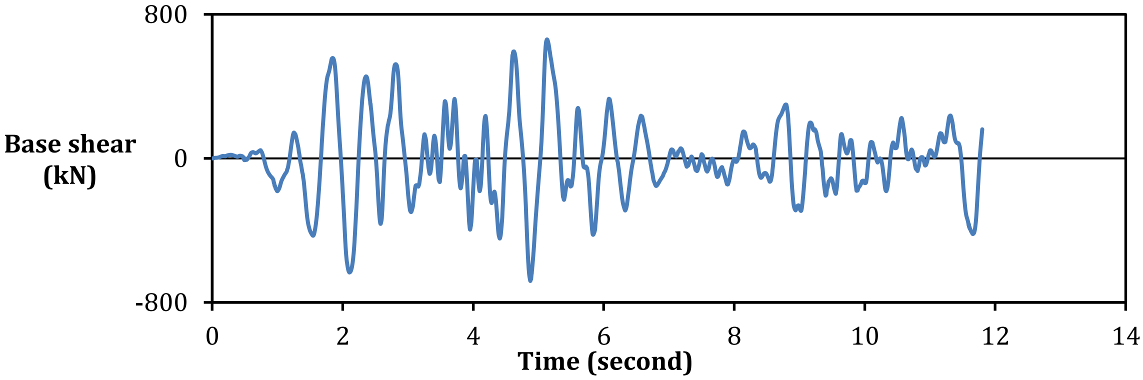

Figure 20. Base shear of model of Frame D under the El Centro 0.32g 1940 NS.

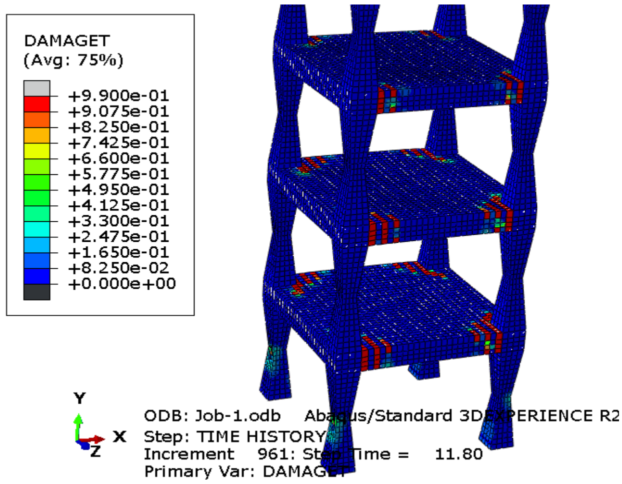

Figure 21. Damages of Frame D under the El Centro 0.32g NS 1940.

In Frame D, the damages mainly occurred in the beams, not in the columns, which agrees with the aforementioned design strategy for earthquake-resistant structures of weak beam-strong column design strategy. Hence, the non-prismatic columns in Frame D enhanced the seismic behavior of the RC frame.

If the effect of the proposed non-prismatic geometry on the behavior of RC columns is to be studied experimentally, scaled-down RC frames can be tested using a shaking table. Base excitation can be applied to each model to evaluate the response of frames with non-prismatic columns and their corresponding reference models with prismatic columns. One-story, two-story, or multi-story scaled frames may be used, depending on the capacity of the shaking table.

5. CONCLUSIONS

The numerical analyses conducted in this study indicate that tapering RC columns, by reducing the cross-sectional dimensions at mid-height and increasing them toward the ends while preserving the overall concrete volume, can enhance the seismic performance of RC frame structures. Based on the behavior of the analyzed models, the following conclusions are drawn:

1- The seismic performance of an RC prismatic column can be significantly improved by tapering it from a smaller cross-section at mid-height to a larger cross-section at the ends. For a tapering angle of 3.814°, the lateral strength increases by 56.4%, and the initial stiffness is enhanced by 50.5%.

2- The overstrength factor of the RC frame with non-prismatic columns, tapered from mid-height toward the ends at an angle of 3.814°, was 56.48% higher than that of the reference frame with prismatic columns

3- The RC tapered columns exhibited better control of lateral displacement, which in turn means improved control of story drift under lateral loads such as earthquake forces. This results in reduced damage to both structural and nonstructural components under the same loading conditions compared to prismatic columns.

4- Under earthquake loading, the RC frame with tapered columns exhibited a more favorable failure mode than the reference frame, as damage was concentrated mainly in the beams rather than the columns. This behavior reflects a desirable strong-column–weak-beam mechanism, enhancing the overall seismic behavior of the structure.

5- The formation of plastic hinges predominantly at the beam ends in the frame with non-prismatic columns indicates a more desirable failure mechanism, contributing to enhanced energy dissipation capacity relative to the reference frame.

6- Since the lateral stiffness of RC frames can be modified by changing the geometry of the columns during the design process, while keeping the overall structural weight unchanged, the natural frequency of the structure can, to some extent, be controlled when necessary.

NOMENCLATURE

Symbol	Description	Symbol	Description
C_s	Seismic response coefficient.	R	Response modification factor.
C_{vx}	Factor of the vertical distribution.	S_{DS}	Design response spectral acceleration, g.
F_x	Force applied at the level x.	V	Total base shear, kN.
h_i	Distance from the base to the level i.	W	Effective seismic weight of the structure, kN.
h_x	Distance from the base to the level x.	w_i	Portion of the total weight at the level i.
I	Importance coefficient.	w_x	Portion of the total weight at the level x.

Acknowledgements

The authors are grateful to the University of Baghdad, College of Engineering, Civil Engineering Department for their support.

Credit Authorship Contribution Statement

Jabbar A. Kadhim: Writing – review & editing, Writing – original draft, Validation, Software, Methodology. Salah R. Al.Zaidee: Writing – review & editing, Software. Hayder A. Al-Baghdadi: Writing – review & editing.

Declaration of Competing Interest

The authors declare that they have no known competing financial interests or personal relationships that could have appeared to influence the work reported in this paper.

REFERENCES

Abbas, R.M., and Abdulhameed, R.A., 2019. Frequency domain analysis for geometric nonlinear seismic response of tall reinforced concrete buildings. *Journal of Engineering*. https://doi.org/10.31026/j.eng.2019.03.09

American Society of Civil Engineers, 2016. Minimum design loads for buildings and other structures (ASCE/SEI 7-16). Reston. https://doi.org/10.1061/9780784414248

Annan, C., Youssef, M., and El Naggar, M., 2008. Assessment of overstrength and ductility of a four-story modular steel building braced frame. *Proceedings of the 2nd Canadian Conference on Effective Design of Structures*, McMaster University, Hamilton, ON, Canada, pp. 20-23.

Arroyo, O., and Gutierrez, S., 2017. A seismic optimization procedure for reinforced concrete framed buildings based on eigenfrequency optimization. *Engineering Optimization*, 49(7), pp. 1166–1182. https://doi.org/10.1080/0305215X.2016.1241779

Bai, J., and Ou, J., 2015. Realization of the global yield mechanism of RC frame structures by redesigning the columns using column tree method. *Science China Technological Sciences*, 58(9), pp. 1627–1637. https://doi.org/10.1007/s11431-015-5875-3

Bai, Y., 2019. *Structural dynamics*. John Wiley & Sons. ISBN: 978-1-119-60560-7.

Balling, R.J., and Yao, X., 1997. Optimization of reinforced concrete frames. *Journal of Structural Engineering*, 123(2), pp. 193–202. https://doi.org/10.1061/(ASCE)0733-9445(1997)123:2(193)

Brant, N., 1984. Reinforced concrete columns of variable cross section. *PhD thesis. City University, Department of Civil Engineering, United Kingdom*.

Chen, H., Xie, Q., Dai, B., Zhang, H., and Chen, H., 2016. Seismic damage to structures in the Ms 6.5 Ludian earthquake. *Earthquake Engineering and Engineering Vibration*, 15(1), pp. 173–186. Available at: https://doi.org/10.1007/s11803-016-0314-4

Chen, W.F. and Lui, E.M., 2005. *Handbook of structural engineering*. CRC press. ISBN: 0-8493-1569-7.

Chopra, A.K., 2012. *Dynamics of structures*. 4th ed. Upper Saddle River, NJ: Prentice Hall. ISBN: 978-0-13-285803-8.

Derecho, A.T. and Kianoush, M.R., 2001. *Seismic design of reinforced concrete structures*. *The seismic design handbook*, Springer, Boston, MA, pp.463-561. https://doi.org/10.1007/978-1-4615-1693-4_10

Dooley, K.L., and Bracci, J.M., 2001. Seismic evaluation of column-to-beam strength ratios in reinforced concrete frames. *Structural Journal*, 98(6), pp. 843–851. https://doi.org/10.14359/10751

Elnashai, A.S. and Di Sarno, L., 2015. *Fundamentals of earthquake engineering: from source to fragility*. John Wiley & Sons. ISBN 978-0-470-02483-6.

Fadaee, M.J., and Grierson, D.E., 1998. Design optimization of 3D reinforced concrete structures having shear walls. *Engineering with Computers*, 14(2), pp. 139–145. https://doi.org/10.1007/BF01213587

Fattah, M.Y., and Al-Tae'e, A.Y., 2004. Seismic conditions in Baghdad region: An evaluation of seismic design forces. *Journal of Engineering*, 10(3), pp. 399–412. https://doi.org/10.31026/j.eng.2004.03.09

Fragiadakis, M., and Papadrakakis, M., 2008. Performance-based optimum seismic design of reinforced concrete structures. *Earthquake Engineering & Structural Dynamics*, 37(8), pp. 825–844. https://doi.org/10.1002/eqe.786

Gharehbaghi, S., Moustafa, A., and Salajegheh, E., 2016. Optimum seismic design of reinforced concrete frame structures. *Computers and Concrete*, 17(6), pp. 761–786. http://dx.doi.org/10.12989/cac.2016.17.6.761

Hu, Y., 2021. Risk-based multiobjective optimal seismic design for RC piers using the response surface method and NSGA-II. *Advances in Civil Engineering*, 2021, P. 8852203. https://doi.org/10.1155/2021/8852203

International Code Council, 2015. International Building Code 2015. 1st ed. Country Club Hills, IL: International Code Council. ISBN: 978-1-60983-468-5.

Jebelli, S.T., and Behnam, B., 2024. Intelligent life cycle cost-based framework for seismic design of conventional structures. *Buildings*, 14(9), P. 2597. https://doi.org/10.3390/buildings14092597

Kadhim, J.A., and Al-Zaidee, S.R., 2023. Validated three-dimensional finite element modeling for static behavior of RC tapered columns. *Journal of the Mechanical Behavior of Materials*, 32(1), pp. 1–10. https://doi.org/10.1515/jmbm-2022-0226

Kadhim, J.A., and Al-Zaidee, S.R., 2024. Numerical simulation for strength and stability of RC tapered columns. *Engineering, Technology & Applied Science Research*, 14(1), pp. 14819–14824. https://doi.org/10.48084/etasr.7228

Kaveh, A., and Zakian, P., 2014. Optimal seismic design of reinforced concrete shear wall-frame structures. *KSCE Journal of Civil Engineering*, 18(7), pp. 2181–2190. https://doi.org/10.1007/s12205-014-0640-x

Kaveh, A., and Zakian, P., 2014. Optimal seismic design of reinforced concrete shear wall-frame structures. *KSCE Journal of Civil Engineering*, 18(7), pp .2181–2190. https://doi.org/10.1007/s12205-014-0640-x

Krishnamoorthy, C., and Munro, J., 1973. Linear program for optimal design of reinforced concrete frames. *Proceedings of IABSE*, 3, pp.119–141.

Mahmoud, T.K., and Al-Baghdadi, H.A., 2018. Seismic response of nonseismically designed reinforced concrete low rise buildings. *Journal of Engineering*, 24, pp. 112–127. https://doi.org/10.31026/j.eng.2018.04.08

Manohar, S., and Madhekar, S., 2015. Seismic design of RC buildings. *Springer Transactions in Civil and Environmental Engineering*. https://doi.org/10.1007/978-81-322-2319-1

Ministry of Construction and Housing, 2017. Iraqi Seismic Code for Buildings: IQS No. 303. Baghdad. Central Organization for Standardization and Quality Control (in Arabic).

Nie, X., Zhang, S., Jiang, T., and Yu, T., 2020. The strong column–weak beam design philosophy in reinforced concrete frame structures: A literature review. *Advances in Structural Engineering*, 23, pp. 3566–3591. https://doi.org/10.1177/1369433220933463.

Sucuoglu, H., and Akkar, S., 2014. Basic earthquake engineering from seismology to analysis and design. *Springer*. https://doi.org/10.1007/978-3-319-01026-7

Sunitha, P., Murty, C., and Goswami, R., 2014. Quantifying parameters that ensure large deformability of earthquake resistant RC building in high seismic regions. *In: 10th US National Conference on Earthquake Engineering Frontiers of Earthquake Engineering*. http://dx.doi.org/10.4231/D3ZK55M8K

Tanhadoust, A., Madhkhan, M., and Daei, M., 2023. Two-stage optimization method for design of reinforced concrete frames using optimal pre-determined section database and non-revisiting genetic algorithm. *Structural and Multidisciplinary Optimization*, 66, P. 255. https://doi.org/10.1007/s00158-023-03709-3

Taranath, B. S., 2004. *Wind and earthquake resistant buildings: Structural analysis and design*. CRC Press. https://doi.org/10.1201/9780849338090

Zakian, P., and Kaveh, A., 2023. Multi-objective seismic design optimization of structures: A review. *Archives of Computational Methods in Engineering*, 31(6), pp. 1–25. https://doi.org/10.1007/s11831-023-09992-z

Zou, X.K., and Chan, C.M., 2004. Seismic drift performance-based design optimization of reinforced concrete buildings. *13th World Conference on Earthquake Engineering, Vancouver, BC, Canada*, August 2004, pp. 1–6.

Zou, X.K., and Chan, C.M., 2005. An optimal resizing technique for seismic drift design of concrete buildings subjected to response spectrum and time history loadings. *Computers & Structures*, 83, pp. 1689–1704. https://doi.org/10.1016/j.compstruc.2004.10.002

الأداء الزلزالي للأعمدة الخرسانية المسلحة متغيرة المقطع

جبار عبدالعالي كاظم*، صلاح رحيمة عبيد، حيدر عامر أحمد

قسم الهندسة المدنية، كلية الهندسة، جامعة بغداد، بغداد، العراق

الخلاصة

تهدف الدراسة الى التحري عن امكانية تحسين الاداء الزلزالي للاعمدة الخرسانية المسلحة من خلال تغيير شكلها من ثابتة الى متغيرة المقطع. نموذجان من الهياكل ثلاثية الطوابق تم تحليلها تحت تاثير احمال عرضية سكونية بعد تسليط حمل الوزن الذاتي لها. أحد النموذجين ذو اعمدة ثابتة المقطع كنموذج مرجعي والاخر بأعمدة متغيرة المقطع. اظهرت نتائج الدراسة ان الاعمدة الخرسانية المسلحة التي يزاح جزء من حجم خرسانتها من وسط العمود باتجاه النهايات يتحسن اداؤها الزلزالي بدلالة قابلية مقاومة قوة القص وبدلالة جساءة المنشأ العرضية. اظهرت الدراسة ان تغيير شكل الأعمدة من ثابتة المقطع الى متغيرة المقطع من الوسط باتجاه النهايات بزاوية ميل 3.814 درجة يزيد المقاومة الجانبية بمقدار 56.4% و الجساءة الابتدائية بنسبة 50.5% و كذلك يزيد عامل تضخيم المقاومة بنسبة 56.48% ، كما اظهرت نتائج التحليل الديناميكي اللاخطي ان الهيكل الخرساني ذا الأعمدة متغيرة المقطع قد تحسن نمط الفشل فيه تحت تاثير هزة ارضية تعجيلها الاقصى 0.32g (El Centro 0.32g NS 1940) مقارنة مع النموذج المرجعي ذي الأعمدة ثابتة المقطع، حيث حصلت التشققات في الاول في الجسور بشكل رئيسي بدلا من الاعمدة و هو كما يتفق مع فلسفة التصميم الانشائي التي تتطلب أعمدة قوية و جسور ضعيفة.

الكلمات المفتاحية: متغيرة المقطع، خرسانة مسلحة، اعمدة، زلزالي، تضرر.